Two Methods for Nonparametric Spectrum Peak Discrimination

Miroslav Zivanovic, Alfonso Carlosena

Universidad Pública de Navarra
Dept. Electrical and Electronic Engineering
Campus de Arrosadía, s/n
E-31006, Pamplona, Spain
Phone/Fax: + 34 948 168 932 / +34 948 169 720
e-mail: miro@tsc.unavarra.es
http://www.tsc.upna.es/Analog/Analog.html

Abstract

The conventional DFT-oriented nonparametric interpolation methods, based on time windowing and the DTFT envelope curve resampling (zero padding, Chirp-z [1], *frequency scale distortion* [2], *etc.), can improve the spectrum computational resolution. Two methods proposed herein involve some modification of the frequency domain representation and apparently improve the spectrum physical resolution.*

Introduction

Peak discrimination is a topic of great importance within spectrum signal processing. Very often, the spectral information provided by the *DFT* simply is not enough to obtain all the details about the spectrum (number of peaks, peak bandwidth, peak central frequency etc.). The reason for this lies in a lack of either physical or computational frequency resolution. The physical frequency resolution, or the Peak Discrimination Limit (*PDL*), refers to the minimum resolvable frequency separation between two sinusoidal signal components close in frequency and is directly related to the mainlobe bandwidth of the time-domain window spectrum [3,4]. On the other hand, computational resolution can smooth the graphical representation of the *DFT* spectrum and resolve possible ambiguities, due to the picket-fence effect, but it is limited by the physical resolution.

The objective of this work is to improve the *PDL* by intervening in the frequency domain and changing the properties of the corresponding interpolated *DFT* spectrum, rather than applying a particular time window to the input sequence. That is, we intent to change the form of the Discrete Time Fourier Transform (*DTFT*) envelope curve, without altering significantly the physical reality. It could be seen as applying a "frequency window" to the input sequence N-point *DFT* spectrum, by interpolating it at only N points in two different ways. However, an interpretation in terms of time window is also possible.

Scaled interpolated DFT spectrum (SIDFT).

An N-point *DFT* spectrum interpolated at N points (padding N zeros to the N-point input sequence) is equivalent to resampling the *DTFT* envelope curve with the resolution $\pi k/N$, k = 0, 1, ..., 2N-1. A single signal component given by

$$x(n) = e^{j\Omega_1 n}\ ,\ \ \Omega_1 = (k+\delta)\Omega_o\ ,\ \ \Omega_o = \frac{2\pi}{N},\ \ \delta \in [0,1],$$

will have a spectrum peak, characterized by the magnitude interplay among the frequency samples $X(k)$, $X(k+1/2)$ and $X(k+1)$. Fig. 1(a) shows that a spectrum peak interpretation of $x(n)$, as a function of δ, is given by a collection of *sincs* separated by π/N.

By scaling $X(k+1/2)$ by a factor a = 0.65, the peak interpretation is obviously modified but its general characteristic is preserved in the following sense:

$$\begin{array}{l} |X(k+1)| < \{ |X(k)|,\ a|X(k+1/2)| \},\ 0<\delta<0.5 \\ |X(k)| < \{ a|X(k+1/2)|,\ |X(k+1)| \},\ 0.5<\delta<1 \end{array}, \qquad (1)$$

which is shown on Fig.1(b). Such a spectrum we call the interpolated scaled spectrum *SIDFT(k)* and it is given as a superposition of two 2N-point spectra:

$$SIDFT(k) \;=\; \begin{array}{c} X_{DFT}(k) = \begin{cases} X(k/2) & ,\ k\ \ even \\ 0 & ,\ k\ \ odd \end{cases} \\ + \\ X_{INT}(k) = \begin{cases} 0 & ,\ k\ \ even \\ aX(k-1/2) & ,\ k\ \ odd \end{cases} \end{array}, \qquad (2)$$

k = 0, 1, ..., 2N - 1. Their corresponding continuos-frequency domain representations will be:

$$X_{DFT}(\Omega) = X(\Omega)P(\Omega) \quad \text{and} \quad X_{INT}(\Omega) = aX(\Omega)P\left(\Omega - \frac{\pi}{N}\right),$$

where Ω is a continuos digital frequency, $X(\Omega)$ is the original sequence *DTFT* spectrum and $P(\Omega)$ is a frequency domain impulse train,

$$P(\Omega) = \sum_m e^{-jmN\Omega}. \tag{3}$$

By using the *IDTFT* we obtain the expressions for their time domain representations respectively:

$$\begin{aligned} x_{DFT}(n) &= \frac{1}{2}\sum_m x(n - mN) \\ x_{INTT}(n) &= \frac{1}{2}a\sum_m (-1)^m x(n - mN) \end{aligned} \tag{4}$$

Expressions (4) can be seen as a periodic extension of the input sequence multiplied by a window shown on the Fig.2.

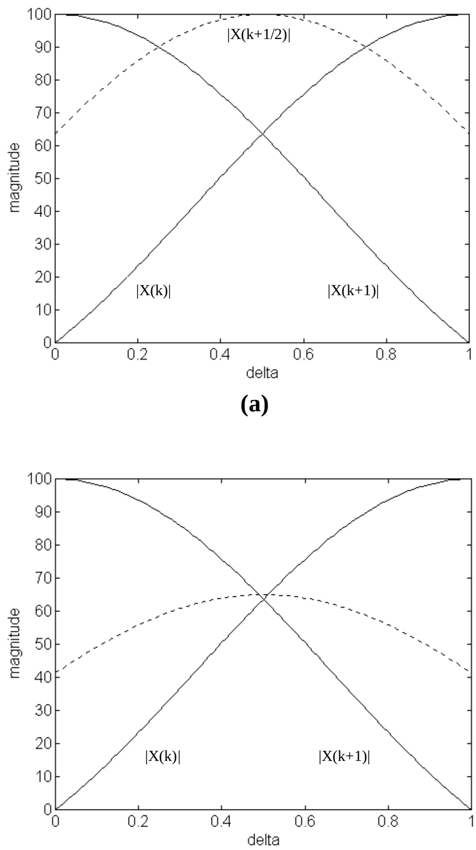

(a)

(b)

Fig. 1 Single spectrum peak interpretation
a) plane *DFT* b) *SDIFT*

It can be seen from (4) that if a = 1, the *SIDFT* time window is the same as the 2N-point *DFT* interpolation window (the original sequence padded by N zeros). The window w_{SIDFT} has smaller equivalent noise bandwidth than the interpolation rectangular window:

$$\begin{aligned} ENBW_{SIDFT} &= N\,\frac{\sum_{n=0}^{2N-1} w_{SIDFT}^2(n)}{\left[\sum_{n=0}^{2N-1} w_{SIDFT}(n)\right]^2} = 0.7113 \\ ENBW_{RECT} &= 1 \end{aligned} \tag{5}$$

This means that the mainlobe bandwidth for w_{SIDFT} will be narrower than that of the rectangular window. Consequently, the *PDL* will reduce, by means of (2), which can be observed in the section of experimental results.

It can be seen that the *PDL* improves principally for $\delta \in [0, 0.5]$. In order to achieve the same objective for the entire interval $\delta \in [0, 1]$ the following modification of the *SIDFT*(k) is proposed:

$$SIDFT^{(1)}(k) = X_{DFT}(k) = \begin{cases} aX(k/2) & , k \text{ even} \\ 0 & , k \text{ odd} \end{cases} + X_{INT}(k) = \begin{cases} 0 & , k \text{ even} \\ X(k - 1/2) & , k \text{ odd} \end{cases}, \tag{6}$$

k = 0, 1, ..., 2N - 1. Hence, the resulting *PDL* for $\delta \in [0, 1]$ is given as

$$PDL = f(\delta) = \min_{0<\delta<1}\left\{PDL \;\; for\ SIDFT,\ PDL \;\; for\ SIDFT^{(1)}\right\} \tag{7}$$

The computational cost is similar to that of the conventionally interpolated *DFT* spectrum and can be implemented in a simple manner, since the scaling factor is a constant.

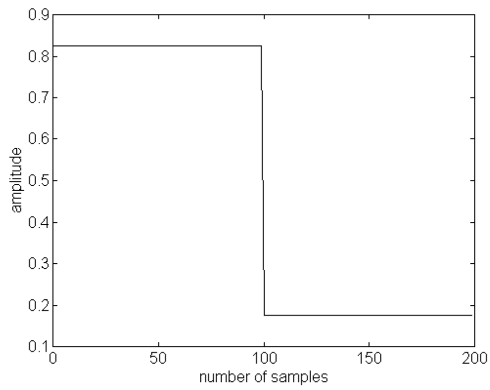

Fig. 2. Interpolation time domain window w_{SIDFT} for the *SIDFT* spectrum for a = 0.65 and N = 100

Linear combination DFT spectrum interpolation

We have seen in the previous section that by resampling the *DTFT* curve at $2N$ points (conventional interpolation) and scaling properly in magnitude, the *DTFT* curve is apparently modified but the peak characteristic is preserved for all δ (1). Here we intent to emulate this result by combining linearly the adjacent samples of the plane N-point *DFT* spectrum for $\delta \in$ [0, 1], rather then resampling the *DTFT* curve, that is,

$$\begin{aligned}\hat{X}(k+1/2) &= C_1 X(k) + C_2 X(k+1) = \\ &= [C_1 X_R(k) + C_2 X_R(k+1)] + j[C_1 X_I(k) + C_2 X_I(k+1)],\end{aligned} \quad (8)$$

where

$$X_R(k) = \mathrm{Re}\{X(k)\}, \qquad X_I(k) = \mathrm{Im}\{X(k)\}$$
$$X_R(k+1) = \mathrm{Re}\{X(k+1)\}, \qquad X_I(k+1) = \mathrm{Im}\{X(k+1)\},$$

$k = 0, 1, ..., N$-1 and C_1, C_2 = Const.

By making use of the least square approximation method, we intent to find the optimum value for C_1 and C_2. From (8) it is necessary to adjust the real and imaginary parts separately, so that their coherent sum match, as close as possible, the $|X(k+1/2)|$ curve given in Fig.1(b). There are two ways to define the approximation function, since interchanging the real and imaginary parts doesn't modify the magnitude representation.

i)

$$\begin{aligned}J_R(C_1, C_2) &= \sum_{0<\delta<1} \{X_R(k+1/2) - C_1 X_R(k) - C_2 X_R(k+1)\}^2 \\ J_I(C_1, C_2) &= \sum_{0<\delta<1} \{X_I(k+1/2) - C_1 X_I(k) - C_2 X_I(k+1)\}^2\end{aligned} \quad (9)$$

From (9) we obtain $C_1 = C_2$ and consequently $C(J_R)$ = 0.33, $C(J_I)$ = - 1.13.

ii) Using the same scheme but defining now the cost functions as

$$\begin{aligned}J_R(C_1, C_2) &= \sum_{0<\delta<1} \{X_R(k+1/2) - C_1 X_I(k) - C_2 X_I(k+1)\}^2 \\ J_I(C_1, C_2) &= \sum_{0<\delta<1} \{X_I(k+1/2) - C_1 X_R(k) - C_2 X_R(k+1)\}^2\end{aligned} \quad (10)$$

gives $C_1 = - C_2$, which implies $C(J_R)$ = 0.50, $C(J_I)$ = - 0.46

Choosing the method *ii*) for being more coherent and bearing in mind the constraint

$$\left|\hat{X}(k+1/2)\right| \geq \left|X(k+1/2)\right| \text{ for } \delta = 0.5,$$

it is finally obtained C = 0.51. Note that the negative value for $C(J_I)$ will not change the resulting magnitude spectrum. The peak interpretation according to the linear combination method is compared to the *SIDFT* in Fig.3.

We stress that the linear combination method can be explained in terms of linear vector space, as the concepts of the *DFT* spectrum and orthogonal vector decomposition are highly related by virtue of inner product [5,6]. Consequently, any kind of the *DFT* spectrum interpolation can be seen as a projection decomposition of a signal vector over the N vectors of the interpolation basis inserted in the N-dimensional orthogonal *DFT* basis [7,8].

Therefore, the following relations between the particular projections and their corresponding interpolation vectors can be established:

$$\begin{aligned}|X(k+1/2)| &\leftrightarrow \boldsymbol{X}(k+1/2) = e^{j\Omega_o(k+1/2)n} \\ |\hat{X}(k+1/2)| &\leftrightarrow \hat{\boldsymbol{X}}(k+1/2) = e^{j\Omega_o kn} - e^{j\Omega_o(k+1)n}\end{aligned} \quad (11)$$

Obviously, those vectors do not coincide in vector space orientation. Nevertheless, according to (11), it is possible to treat $\hat{\boldsymbol{X}}$ (k+1/2) as if it lied in the plane defined by the vectors $\boldsymbol{X}(k)$ and $\boldsymbol{X}(k+1)$, orthogonal to each of the planes of the N-dimensional *DFT* vector space. This property implies that all vectors of the *DFT* basis, with exception of $\boldsymbol{X}(k)$ and $\boldsymbol{X}(k+1)$, will have zero projection onto $\hat{\boldsymbol{X}}$ (k+1/2). This leads to the concept of frequency scaling, similar to the *SIDFT*. Like (7), it is necessary to repeat the algorithm in the following sense:

$$\hat{X}(k) = 0.51[X(k-1/2) - X(k+1/2)]. \quad (11)$$

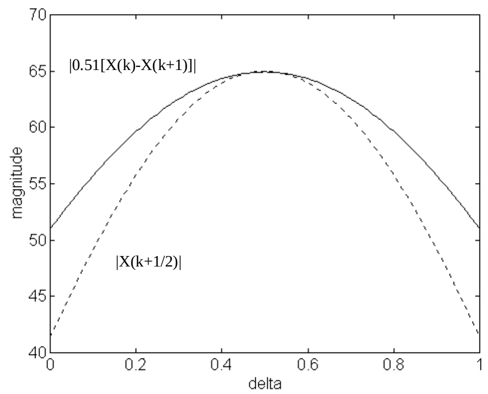

Fig. 3. A single peak interpretation:
dotted line - *SIDFT* spectrum;
continuous line - linear combination spectrum

Experimental results

A signal formed by two components close in frequency was treated, that is,

$$x(n) = A_1 e^{j\Omega_1 n} + A_2 e^{j\Omega_2 n}, \quad \Omega_1 - \Omega_2 < \Omega_o.$$

Only the two largest frequency samples are being applied the *SIDFT* method in order to avoid altering the dynamic of the rest of the spectrum. The PDL is investigated for $\delta \in$ [0, 0.5], having a magnitude difference ΔA as a parameter, in the following way:

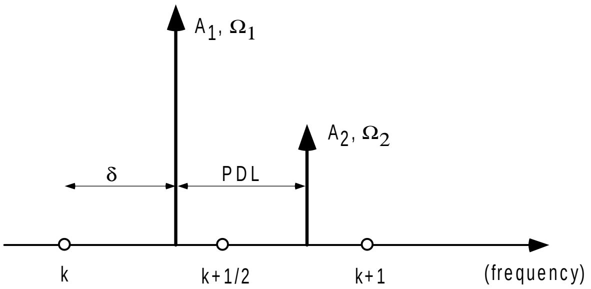

From Fig.4 it can be seen that the *SIDFT* is more effective when the magnitude difference is smaller. For larger magnitude difference, the discrimination process is corrupted by the "short term" leakage effect.

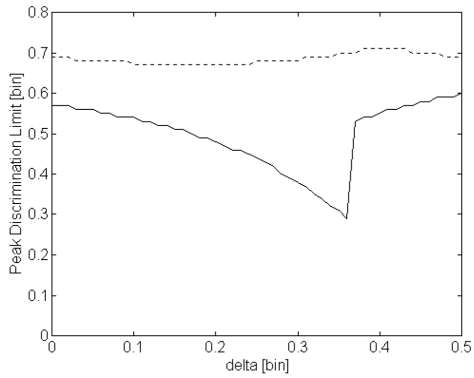

(a) $\Delta A = 0$

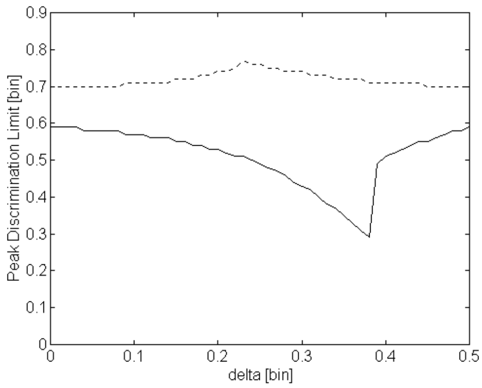

(b) $A_2 = 0.8A_1$

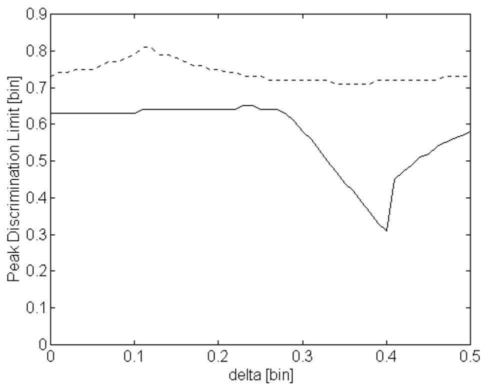

(c) $A_2 = 0.6A_1$

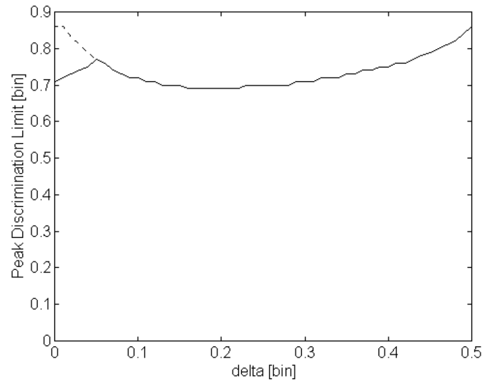

(d) $A_2 = 0.4A_1$

Fig. 4. The Peak discrimination limit for:
conventional interpolation - dotted line
SIDFT interpolation - solid line

Conclusions

Two methods for nonparametric spectrum peak discrimination are presented. They are based on the apparent reduction of the corresponding frequency window mainlobe bandwidth by scaling/combining the largest spectrum samples. The equivalent time domain window in the case of the *SIDFT* is also presented. Finally, a comparison of different methods, including the conventional interpolation, is given in a graphical form.

References

[1] L. R. Rabiner, R. W. Schafer and C M. Rader, "The chirp-z transform algorithm", IEEE Trans. Audio Electroacoust., vol. 17, pp. 86-92, June 1969.

[2] A. V. Oppenheim, D. H. Johnson, "Discrete representation of signals", Proc. IEEE, vol 60, pp. 681-691, June 1972

[3] F. J. Harris, "On the use of windows for harmonic analysis with the Discrete Fourier Transform", IEEE Proc. vol. 66, no. 1, January 1978

[4] S. Gade and H. Herlufsen, "Windows to FFT analysis, part I and II", Bruel & Kjaer tech. rew., no. 4., 1987

[5] S. K. Berberian, "Introduction to Hilbert spaces", Oxford University Press, Inc, 1961

[6] E. Masry, K. Steiglitz and B. Liu, "Bases in Hilbert space related to the representation of stationary operators", SIAM Jou. of App. Math. vol. 16, Nº. 3, May 1968

[7] G. Sansone, "Orthogonal functions", Dover Publications, Inc., New York 1991

[8] H. F. Davis, "Fourier series and orthogonal functions", Dover Publications, Inc., New York 1989